Contribution from the Department of Chemistry,
University of South Carolina, Columbia, South Carolina 29208

Cluster Synthesis. 25. Synthesis and Characterization of New Mixed-Metal Cluster Complexes by Metal–Metal Exchange. Reactions of the Sulfido Cluster Complexes $M_3(CO)_9(\mu_3\text{-}CO)(\mu_3\text{-}S)$ (M = Fe, Ru, and Os) with $W(CO)_5L$ (L = CO or PMe_2Ph)

Richard D. Adams,* James E. Babin, Pradeep Mathur, K. Natarajan, and Jin-Guu Wang

Received August 3, 1988

The reactions of the sulfur-bridged metal carbonyl cluster complexes $M_3(CO)_9(\mu_3\text{-}CO)(\mu_3\text{-}S)$ (M = Fe (**1a**); M = Ru (**1b**); M = Os (**1c**)) with $W(CO)_6$ and $W(CO)_5(PMe_2Ph)$ in the presence of UV irradiation have yielded the new mixed-metal cluster complexes $M_2W(CO)_{10}L(\mu_3\text{-}S)$ (M = Fe, L = CO (**2**) (21%); M = Fe, L = PMe_2Ph (**2a**) (42%); M = Ru, L = PMe_2Ph (**2b**) (47%); M = Os, L = PMe_2Ph (**2c**) (10%)) and $Os_3W(CO)_{11}(PMe_2Ph)_2(\mu_3\text{-}S)$ (**3c**) (13%). The reaction of $Os_4(CO)_{12}(\mu_3\text{-}S)$ (**4**) with $W(CO)_5(PMe_2Ph)$ in the presence of UV irradiation has yielded the new mixed-metal cluster complex $Os_4W(CO)_{15}(PMe_2Ph)(\mu_3\text{-}S)$ (**5**). Compounds **2**, **2a**, **3c**, and **5** were characterized by single-crystal X-ray diffraction analyses. Crystal data for **2**: space group $P2_1/n$, a = 9.247 (2) Å, b = 12.638 (3) Å, c = 14.382 (2) Å, β = 90.86 (1)°, Z = 4, R_F = 0.028, R_{wF} = 0.034. Crystal data for **2a**: space group $P2_1/c$, a = 10.454 (4) Å, b = 13.302 (4) Å, c = 17.532 (3) Å, β = 104.01 (2)°, Z = 4, R_F = 0.025, R_{wF} = 0.027. Crystal data for **3c**: space group, $P2_1/n$, a = 14.646 (4) Å, b = 12.669 (2) Å, c = 19.377 (4) Å, β = 106.22 (2)°, Z = 4, R_F = 0.040, R_{wF} = 0.041. Crystal data for **5**: space group $P\bar{1}$, a = 10.713 (1) Å, b = 11.814 (2) Å, c = 14.471 (2) Å, α = 94.36 (2)°, β = 105.879 (9)°, γ = 86.12 (1)°, Z = 2, R_F = 0.029, R_{wF} = 0.036. Compounds **2** and **2a** are sulfur-bridged trinuclear cluster complexes consisting of two irons with three carbonyl ligands each and one tungsten atom with five ligands. The sulfur–tungsten and two tungsten–iron bonds are formulated as donor–acceptor bonds. The tungsten–iron bonds in **2a** are 0.038 Å shorter than those in **2**. This is attributed to the formation of stronger tungsten–iron bonds due to a greater availability of electron density on the tungsten atom of **2a** as compared to that of **2**. Compound **3c** contains a tetrahedral arrangement of three osmium atoms and one tungsten atom with a triply bridging sulfido ligand on one of the Os_2W triangles. Compound **5** consists of a tetrahedral cluster of three osmium atoms and one tungsten atom with an $Os(CO)_3$ group bridging one of the osmium–osmium edges of the cluster and a sulfido ligand bridging one of the tungsten–osmium edges and extending to the edge-bridging $Os(CO)_3$ group.

Introduction

It is now well established that bridging ligands can play an important role, both in the stabilization and in the formation of metal cluster complexes.[1-4] The synthesis of mixed-metal cluster complexes by the process of metal–metal exchange usually involves a sequence of two steps, consisting of a metal addition followed by a metal elimination. Occasionally, the addition products can be isolated and provide useful information about the course of the reaction.[5]

We have recently demonstrated the importance of sulfido ligands in cluster syntheses[4] and in their participation in the addition–elimination processes of metal–metal exchange reactions.[6-10] We have now extended these studies to include the synthesis of a series of sulfido–tungsten cluster complexes containing each of the group VIII elements Fe, Ru, and Os. These results are reported here.

Experimental Section

Although the reagents and starting materials are air stable, all reactions were performed under a dry nitrogen atmosphere. Reagent grade solvents were dried over molecular sieves and were deoxygenated with N_2 prior to use. PMe_2Ph and $(CH_2)_2S$ were purchased from Aldrich. The $(CH_2)_2S$ was vacuum distilled before use. Photolysis experiments were performed by using an external high-pressure mercury lamp on reaction solutions contained in Pyrex glassware. IR spectra were recorded on a Nicolet 5-DXB FT-IR spectrophotometer. ^1H NMR spectra were run on a Bruker AM-300 spectrometer operating at 300 MHz. TLC separations were performed on plates (0.25 mm Kieselgel 60 F_{254}, E. Merck). $W(CO)_6$ was purchased from Strem Chemicals, Newburyport, MA, and was sublimed before use. $W(CO)_5(PMe_2Ph)$, $Ru_3(CO)_9(\mu_3\text{-}CO)(\mu_3\text{-}S)$ (**1b**)[11] and $Os_4(CO)_{12}(\mu_3\text{-}S)$ (**4**)[12] were prepared by reported procedures. Elemental analyses were performed by Desert Analytics, Tuscon, AZ.

Preparations of $Fe_3(CO)_9(\mu_3\text{-}CO)(\mu_3\text{-}S)$ and $Os_3(CO)_9(\mu_3\text{-}CO)(\mu_3\text{-}S)$. A 50-mg (0.099-mmol) sample of $Fe_3(CO)_{12}$ was dissolved in 50 mL of hexane. The solution was heated to reflux, and 18 μL (0.248 mmol) of $(CH_2)_2S$ was added. The solution was refluxed under nitrogen for 20 min. The solvent was removed in vacuo, and the residue was chromatographed by TLC with a 1/9 CH_2Cl_2/hexane solvent mixture. This yielded, in order of elution, the following: reddish brown $Fe_3(CO)_9(\mu_3\text{-}S)_2$,[13] 8.4 mg (18%); green $Fe_3(CO)_{12}$, 1.5 mg; brown $Fe_3(CO)_9(\mu_3\text{-}CO)(\mu_3\text{-}S)$ (**1a**), 27 mg (57%). The IR spectrum of **1a** was the same as that reported previously.[14a]

$Os_3(CO)_9(\mu_3\text{-}CO)(\mu_3\text{-}S)$ (**1c**) was obtained in 42% yield by the reaction of $Os_3(CO)_{10}(NCMe)_2$ with an equimolar amount of $(CH_2)_2S$ at 25 °C in 30 min. It was spectroscopically identical with that reported previously.[14b]

Preparation of $Fe_2W(CO)_{11}(\mu_3\text{-}S)$ (2). A 20-mg sample of **1a** (0.042 mmol) was dissolved in 30 mL of hexane. Then, 25 mg of $W(CO)_6$ (0.071 mmol) was added, and the stirred solution was irradiated under a continuous purge of nitrogen for 50 min. The solvent was removed in vacuo, and the residue was chromatographed by TLC on a silica gel with a 95/5 hexane/CH_2Cl_2 solvent mixture. This yielded $Fe_2(CO)_6(\mu\text{-}S)_2$, 0.10 mg; **1a**, 0.2 mg; $Fe_4(CO)_{11}(\mu_4\text{-}S)_2$,[15] 0.2 mg; and black-brown **2**, 5.5 mg (21%). Anal. Calcd: C, 20.88. Found: C, 20.53.

Preparation of $Fe_2W(CO)_{10}(PMe_2Ph)(\mu_3\text{-}S)$ (2a). A 26-mg (0.054-mmol) sample of **1a** was dissolved in 50 mL of hexane solvent. Then, 25 mg (0.054 mmol) of $W(CO)_5(PMe_2Ph)$ was added, and the solution was irradiated under a continuous purge with N_2 for 1 h. The solvent was removed in vacuo, and the residue was chromatographed by TLC with a 1/9 CH_2Cl_2/hexane solvent mixture. This yielded, in order of elution, the following: reddish brown $Fe_3(CO)_9(\mu_3\text{-}S)_2$,[13] 3.0 mg (11%); reddish brown **2a**, 17.1 mg (42%). Anal. Calcd for **2a**: C, 28.99; H, 1.49. Found: C, 29.01; H, 1.36.

Preparation of $Ru_2W(CO)_{10}(PMe_2Ph)(\mu_3\text{-}S)$ (2b). A solution of 20 mg (0.0325 mmol) of **1b** and 45 mg (0.0975 mmol) of $W(CO)_5(PMe_2Ph)$ in hexane solvent was irradiated under a continuous purge with nitrogen

(1) Huttner, G.; Knoll, K. *Angew. Chem., Int. Ed. Engl.* **1987**, *26*, 743.
(2) Roberts, D. A.; Geoffroy, G. L. In *Comprehensive Organometallic Chemistry*; Wilkinson, G., Stone, F. G. A., Abel, E., Eds.; Pergamon: Oxford, England, 1982; Chapter 40.
(3) Vahrenkamp, H. *Adv. Organomet. Chem.* **1983**, *22*, 169.
(4) Adams, R. D. *Polyhedron* **1985**, *4*, 2003.
(5) Richter, F.; Müller, M.; Gartner, N.; Vahrenkamp, H. *Chem. Ber.* **1984**, *117*, 2438.
(6) Adams, R. D.; Babin, J. E.; Wang, J. G.; Wu, W. *Inorg. Chem.*, in press.
(7) Adams, R. D.; Babin, J. E.; Tasi, M. *Organometallics* **1988**, *7*, 219.
(8) Adams, R. D.; Babin, J. E.; Mahtab, R.; Wang, S. *Inorg. Chem.* **1986**, *25*, 1623.
(9) Adams, R. D.; Horváth, I. T.; Wang, S. *Inorg. Chem.* **1986**, *25*, 1617.
(10) Adams, R. D.; Hor, T. S. A. *Inorg. Chem.* **1984**, *23*, 4723.
(11) Adams, R. D.; Babin, J. E.; Tasi, M. *Inorg. Chem.* **1986**, *25*, 4514.
(12) Adams, R. D.; Yang, L. W. *J. Am. Chem. Soc.* **1982**, *104*, 4115.
(13) King, R. B. *Inorg. Chem.* **1963**, *2*, 326.
(14) (a) Markó, L. *J. Organomet. Chem.* **1980**, *190*, C67. (b) Adams, R. D.; Horváth, I. T.; Kim, H. S. *Organometallics* **1984**, *3*, 548.
(15) Adams, R. D.; Babin, J. E.; Estrada, J.; Hall, M. B.; Low, A. A.; Wang, J. G. *Polyhedron*, in press.

0020-1669/89/1328-1440$01.50/0

Table I. Data for the Structural Analyses for Compounds **2**, **2a**, **3**, and **5**

	2	2a	3c	5
		Crystallographic Data		
formula	$WFe_2SO_{11}C_{11}$	$WFe_2SPO_{10}C_{18}H_{11}$	$WOs_3SP_2O_{11}C_{27}H_{22}$	$WOs_4SPO_{15}C_{23}H_{11}\cdot CH_2Cl_2$
temp (±3) °C	23	23	23	23
space group	$P2_1/n$, No. 14	$P2_1/c$, No. 14	$P2_1/n$, No. 14	$P\bar{1}$, No. 2
a, Å	9.247 (2)	10.454 (4)	14.646 (4)	10.713 (1)
b, Å	12.638 (3)	13.302 (4)	12.669 (2)	11.814 (2)
c, Å	14.382 (2)	17.532 (3)	19.377 (4)	14.471 (2)
α, deg	90.0	90.0	90.0	94.36 (2)
β, deg	90.86 (1)	104.01 (2)	106.22 (2)	105.879 (9)
γ, deg	90.0	90.0	90.0	86.12 (1)
V, Å^3	1680.6 (6)	2365 (1)	3452 (1)	1754.5 (9)
M_r	635.72	745.86	1370.9	1534.9
Z	4	4	4	2
ρ_{calc}, g/cm^3	2.51	2.09	2.64	3.07
		Treatment of Data		
abs cor	empirical	empirical	empirical	analytical
abs coeff cm^{-1}	91.4	65.8	146.1	181.0
transmissn coeff: max, min	1.00, 0.38	1.00, 0.72	1.00, 0.16	0.130, 0.033
final residuals: R_F, R_{wF}	0.028, 0.034	0.025, 0.027	0.040, 0.041	0.029, 0.036

for 20 min. The solvent was removed in vacuo, and the residue was separated by TLC. Elution with hexane/CH_2Cl_2 (85/15) yielded, in order of elution, the following: $Ru_3(CO)_{12}$, 0.6 mg; yellow-orange **2b**, 12.7 mg (47%); a trace of dark brown $Ru_5(CO)_{13}(PMe_2Ph)_2(\mu_4\text{-}S)$ (**6**), 0.5 mg. Anal. Calcd for **2b**: C, 25.85; H, 1.33. Found: C, 25.81; H, 1.23. Anal. Calcd for **6**: C, 29.57; H, 1.88. Found: C, 29.27; H, 1.50.

Preparation of $Os_2W(CO)_{10}(PMe_2Ph)(\mu_3\text{-}S)$ (2c) and $Os_3W(CO)_{11}(PMe_2Ph)_2(\mu_3\text{-}S)$ (3c). A 40-mg (0.045-mmol) sample of **1c** and 62.8 mg (0.136 mmol) of $W(CO)_5(PMe_2Ph)$ were dissolved in hexane solvent and irradiated under a continuous purge with nitrogen for 1 h. The solvent was removed in vacuo, and the residue was chromatographed by TLC on silica gel with a 75/25 hexane/CH_2Cl_2 solvent mixture. This yielded, in order of elution, the following: yellow $Os_3(CO)_9(\mu_3\text{-}S)_2$,[16] 1.0 mg (2.5%); orange $Os_4(CO)_{13}(\mu_3\text{-}S)_2$,[17] 5.2 mg (9.7%); yellow **2c**, 4.6 mg (10%); dark brown $Os_3W(CO)_{11}(PMe_2Ph)_2(\mu_3\text{-}S)$ (**3c**), 8 mg (13%). Anal. Calcd for **2c**: C, 21.31; H, 1.09. Found: C, 20.84; H, 1.05. Anal. Calcd for **3c**: C, 23.66; H, 1.62. Found: C, 24.21; H, 1.42.

Preparation of $Os_4W(CO)_{15}(PMe_2Ph)(\mu_3\text{-}S)$ (5). A hexane solution (50 mL) of **4** (16 mg, 0.0153 mmol) and $W(CO)_5(PMe_2Ph)$ (13 mg, 0.0281 mmol) was irradiated under a slow nitrogen purge for 1 h. The solvent was removed in vacuo, and the reddish brown residue was dissolved in a minimum quantity of CH_2Cl_2, transferred to silica TLC plates, and eluted with a 15/85 CH_2Cl_2/hexane solvent mixture. This yielded, in order of elution, the following: $W(CO)_5(PMe_2Ph)$, 4 mg; **4**, 2 mg; orange $Os_4(CO)_{11}(PMe_2Ph)(\mu_4\text{-}S)$,[18] 4 mg (29%); orange-brown **5**, 4 mg (29%).

Crystallographic Analyses

Opaque dark brown crystals of **2** and **2a** were grown by slow evaporation of solvent from a hexane solution at −20 and +5 °C, respectively. Opaque dark brown crystals of both **3c** and **5** were grown by cooling solutions in a hexane/CH_2Cl_2 solvent mixture to −20 °C. The data crystals were mounted in thin-walled glass capillaries. Diffraction measurements were made on a Rigaku AFC6 automatic diffractometer by using graphite-monochromatized Mo Kα radiation. Unit cells were determined and refined from 25 randomly selected reflections obtained by using the AFC6 automatic search, center, index, and least-squares routines. Crystal data, data collection parameters, and results of the analyses are listed in Table I. All data processing was performed on a Digital Equipment Corp. MICROVAX II computer by using the TEXSAN structure solving program library (version 2.0) obtained from Molecular Structure Corp., College Station, TX. Neutral-atom scattering factors were obtained from the standard sources.[19a] Anomalous dispersion corrections were applied to all non-hydrogen atoms.[19b] Full-matrix least-squares of refinements minimized the function

$$\sum_{hkl} w(|F_o| - |F_c|)^2$$

where $w = 1/\sigma(F)^2$, $\sigma(F) = \sigma(F_o^2)/2F_o$, and $\sigma(F_o^2) = [\sigma(I_{raw})^2 + (PF_o^2)^2]^{1/2}/Lp$.

For **2**, the monoclinic space group $P2_1/n$ was established from systematic absences observed in the data. The structure was solved by a combination of direct methods (MITHRIL) and difference Fourier techniques. All atoms were refined with anisotropic thermal parameters.

Compound **2a** crystallizes in the monoclinic crystal system. The space group $P2_1/c$ was established from the systematic absences observed in the data. The positions of the metal atoms were determined by direct methods. All other atom positions were obtained by subsequent difference Fourier syntheses. All non-hydrogen atoms were refined with anisotropic thermal parameters. Hydrogen atom positions were calculated and were included in the structure factor calculations, but they were not refined.

Compound **3c** crystallizes in the monoclinic crystal system. The space group $P2_1/n$ was determined by the absences observed in the data. The structure was solved by a combination of direct methods and difference Fourier techniques. All atoms larger than oxygen were refined with anisotropic thermal parameters. Hydrogen atoms were ignored. The results reported here have been upgraded from our preliminary report[20] by recollecting the data on the same crystal but by using our Rigaku diffractometer equipped with a high-intensity X-ray source and refining with the TEXSAN programs. This analysis is believed to be considerably improved.

Compound **5** crystallizes in the triclinic crystal system with 1 equiv of CH_2Cl_2/formula equiv of **5**. The space group $P\bar{1}$ was assumed and confirmed by the successful solution and refinement of the structure. The structure was solved by a combination of direct methods and difference Fourier techniques. All non-hydrogen atoms were refined with anisotropic thermal parameters. Hydrogen positions were calculated and included in the structure factor calculations, but their positions were not refined.

Results and Discussion

The reactions of the sulfur-bridged metal carbonyl clusters $M_3(CO)_9(\mu_3\text{-}CO)(\mu_3\text{-}S)$ (M = Fe (**1a**);[21] M = Ru (**1b**);[22] M = Os (**1c**)[14b]) with $W(CO)_6$ and $W(CO)_5(PMe_2Ph)$ in the presence of UV irradiation have yielded the new mixed-metal cluster complexes $M_2W(CO)_{10}L(\mu_3\text{-}S)$ (M = Fe, L = CO (**2**) (21%); M = Fe, L = PMe_2Ph (**2a**) (42%); M = Ru, L = PMe_2Ph (**2b**) (47%); M = Os, L = PMe_2Ph (**2c**) (10%)) by metal–metal exchange reactions (eq 1). The ruthenium and osmium homologues of **2** were not obtained, and it is believed that the presence of the phosphine ligand on the tungsten atom stabilizes complexes **2b** and **2c** enough to permit their isolation. This is also supported by a comparison of the molecular structures of **2** and **2a** as determined crystallographically; see below. IR and ^1H NMR spectra of the products, listed in Table II, are fully consistent with the molecular structures, as found in the solid state. Only from the

(16) Goudsmit, R. J.; Johnson, B. F. G.; Lewis, J.; Raithby, P. R.; Whitmire, K. H. *J. Chem. Soc., Chem. Commun.* **1982**, 640.
(17) Adams, R. D.; Horváth, I. T.; Mathur, P.; Segmuller, B. E.; Yang, L. W. *Organometallics* **1983**, *2*, 1078.
(18) This side product was spectroscopically identical with one that was obtained directly from the reaction of **4** with PMe_2Ph.
(19) *International Tables for X-ray Crystallography*; Kynoch Press: Birmingham, England, 1975; Vol. IV: (a) Table 2.2B, pp 99–101; (b) Table 2.3.1, pp 149–150.
(20) Adams, R. D.; Hor, T. S. A.; Mathur, P. *Organometallics* **1984**, *3*, 634.
(21) Markó, L.; Madach, T.; Vahrenkamp, H. *J. Organomet. Chem.* **1980**, *190*, C67.
(22) Adams, R. D.; Babin, J. E.; Tasi, M. *Organometallics* **1988**, *7*, 219.

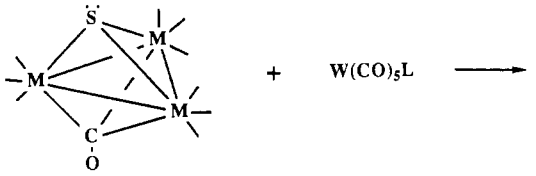

1a, M = Fe
1b, M = Ru
1c, M = Os

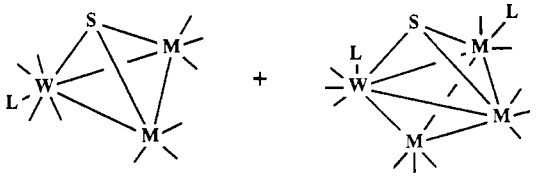

2, M = Fe; L = CO
2a, M = Fe; L = PMe_2Ph
2b, M = Ru; L = PMe_2Ph
2c, M = Os; L = PMe_2Ph

3c, M = Os; L = PMe_2Ph

(1)

preparation of **2c** was a higher nuclearity mixed-metal cluster complex obtained. This was identified as $Os_3W(CO)_{11}(PMe_2Ph)_2(\mu_3\text{-}S)$ (**3c**) on the basis of a crystallographic characterization. From the preparation of **2b**, a very small amount of the pentanuclear ruthenium cluster complex $Ru_5(CO)_{13}(PMe_2Ph)_2(\mu_4\text{-}S)$ (**6**) was obtained.[23] This was found to have

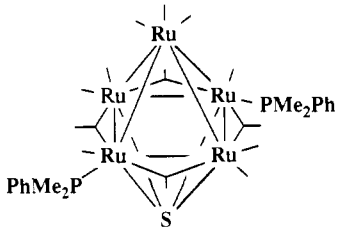

6

a structure analogous to that of $Ru_5(CO)_{11}(\mu\text{-}CO)_4(\mu_4\text{-}S)$ which has four edge-bridging carbonyl ligands.[24]

The reaction of $Os_4(CO)_{12}(\mu_3\text{-}S)$ (**4**) with $W(CO)_5(PMe_2Ph)$ in the presence of UV irradiation was also investigated, and the only mixed-metal cluster complex that was obtained was the expanded cluster $Os_4W(CO)_{15}(PMe_2Ph)(\mu_3\text{-}S)$ (**5**) (eq 2). Small amounts of an orange product believed to be a phosphine derivative of **4** were also obtained from this reaction.[18]

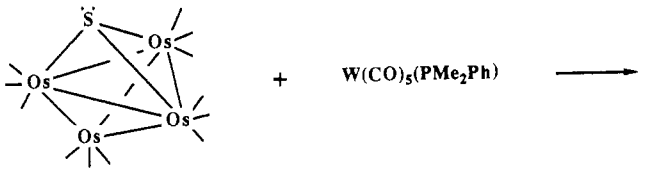

4

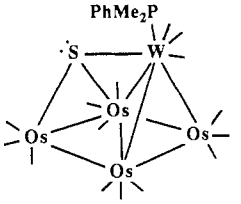

5

(2)

Description of the Structures. ORTEP drawings of the molecular structures of **2** and **2a**, as found in the solid state, are shown in Figures 1 and 2, respectively. Intramolecular bond distances and

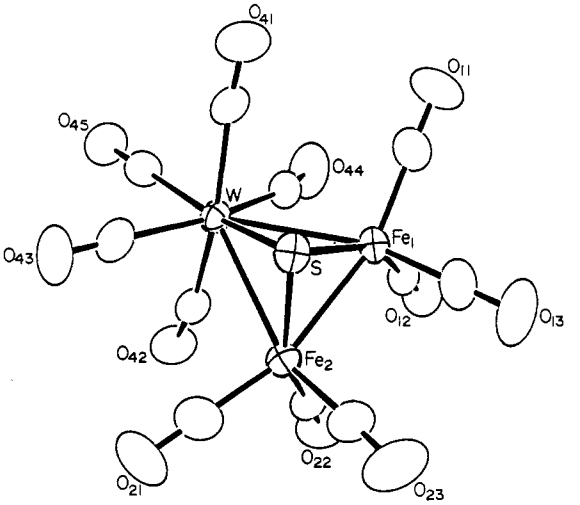

Figure 1. ORTEP drawing of $Fe_2W(CO)_{11}(\mu_3\text{-}S)$ (**2**).

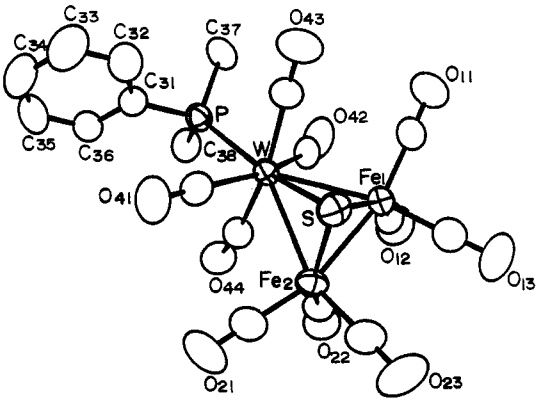

Figure 2. ORTEP drawing of $Fe_2W(CO)_{10}(PMe_2Ph)(\mu_3\text{-}S)$ (**2a**).

angles for **2** and **2a** are listed in Tables III–VI, respectively. Both compounds consist of sulfur-bridged triangular clusters with two iron atoms and one tungsten atom. Compound **2a** is simply a PMe_2Ph derivative of **2** and has the PMe_2Ph ligand located on the tungsten atom in a position approximately *trans* to the bridging sulfido ligand; S–W–P = 160.78 (6)°. Within experimental error the iron–iron bond distances in the two compounds are equal: 2.569 (2) and 2.572 (1) Å. The tungsten–iron distances in a given molecule are equal: 2.854 (1) and 2.852 (1) Å in **2**, and 2.812 (1) and 2.818 (1) Å in **2a**. However, those in **2a** are significantly shorter, 0.038 Å, than those in **2**. If the bond length–bond strength correlation is valid, then this would imply that the W–Fe bonds in **2a** are slightly stronger than those in **2**. The Fe–S bond lengths in **2** and **2a** are not significantly different, 2.180 (2) and 2.179 (2) Å vs 2.196 (2) and 2.178 (2) Å, but the W–S distance in **2a**, 2.406 (2) Å, appears to be significantly shorter than that in **2**, 2.429 (2) Å. The M–C and C–O distances of the carbonyl ligands are normal and not significantly different between the two compounds. In both compounds two of the carbonyl ligands on the tungsten atom, C(42)–O(42) and C(44)–O(44), exhibit a weak semibridging character. There are very few examples of cluster complexes that contain $M(CO)_5$ groups where M = Cr, Mo, and W.[25-27] For the complexes $[M_2Ni_3(CO)_{16}]^{2-}$ (M = Cr, Mo, W[25]) and $MOs_2(CO)_{11}(L)_2$[26] (M = Mo and W, L = $P(OMe)_3$; M = Cr, L = PMe_3), delocalized bonding schemes were proposed to explain the structural character of the coordinated $M(CO)_5$

(23) Compound **6** was also characterized crystallographically: space group $P2_1/n$, a = 12.531 (9) Å, b = 19.659 (12) Å, c = 15.000 (13) Å, β = 94.47 (6)°, Z = 4. R = 0.046 for 3031 reflections.

(24) Adams, R. D.; Babin, J. E.; Tasi, M. *Organometallics* **1988**, *7*, 503.

(25) Ruff, J.; White, R. P., Jr.; Dahl, L. F. *J. Am. Chem. Soc.* **1971**, *93*, 2159.

(26) (a) Davis, H. B.; Einstein, F. W. B.; Johnston, V. J.; Pomeroy, R. K. *J. Am. Chem. Soc.* **1988**, *110*, 4451. (b) Davis, H. B.; Einstein, F. W. B.; Johnston, V. J.; Pomeroy, R. K. *J. Organomet. Chem.* **1987**, *319*, C25.

(27) Barr, R. D.; Green, M.; Howard, J. A. K.; Marder, T. B.; Stone, F. G. A. *J. Chem. Soc., Chem. Commun.* **1983**, 759.

Table II. IR and ^1H NMR Spectra

compd	IR (ν(CO) in hexane), cm^{-1}	^1H NMR (in $CDCl_3$), δ
2	2104 w, 2069 sh, 2059 vs, 2052 sh, 2040 vs, 2030 s, 2010 m, 1995 w, 1982 vw, 1953 w, 1941 w, 1933 sh	
2a	2079 w, 2043 s, 2035 sh, 2022 s, 2009 m, 1997 s, 1976 m, 1964 m, 1895 m, 1878 w	7.44–7.54 (m, 5 H), 2.14 (d, 6 H, J_{P-H} = 9.2 Hz)
2b	2084 m, 2070 w, 2049 vs, 2043 vs, 2021 w, 2007 vs, 1993 m, 1981 m, 1875 m, 1856 m	7.50 (m, 5 H), 2.11 (d, 6 H, J_{P-H} = 9.2 Hz)
2c	2085 w, 2052 s, 2042 vs, 2013 m, 2000 vs, 1980 m, 1969 m, 1878 w, 1862 w	7.46–7.59 (m, 5 H), 2.13 (d, 6 H, J_{P-H} = 9.3 Hz)
3c	2070 m, 2063 sh, 2030 w, 2009 sh, 1996 vs, 1970 w, 1946 w, 1932 vw, 1911 w	7.47 (m, 10 H), 2.21 (d, 3 H, J_{P-H} = 10.4 Hz), 2.19 (d, 3 H, J_{P-H} = 10.1 Hz), 2.12 (d, 3 H, J_{P-H} = 9.0 Hz), 2.06 (d, 3 H, J_{P-H} = 9.3 Hz)
5	2096 w, 2065 vs, 2049 s, 2035 s, 2017 m, 1999 m, 1985 m, 1970 w, 1917 w, 1895 m	7.50 (m, 5 H), 2.24 (d, 3 H, J_{P-H} = 10.3 Hz), 2.07 (d, 3 H, J_{P-H} = 9.3 Hz)
6	2063 m, 2033 vs, 2016 s, 2011 sh, 1985 sh, 1954 w, 1835 m, br	7.30–7.40 (m, 10 H), 1.89 (d, 12 H, J_{P-H} = 9.5 Hz)
7	2096 w, 2088 m, 2068 w, 2053 s, 2040 s, 2009 s, 1997 m, 1981 sh, 1968 w, 1958 vw, 1937 w	

Table III. Intramolecular Distances (Å) for $Fe_2W(CO)_{11}(\mu_3\text{-}S)$ (**2**)

W–C(42)	2.03 (1)	Fe(1)–C(11)	1.79 (1)
W–C(45)	2.04 (1)	Fe(1)–C(12)	1.82 (1)
W–C(44)	2.06 (1)	Fe(1)–S	2.180 (2)
W–C(41)	2.06 (1)	Fe(1)–Fe(2)	2.569 (2)
W–C(43)	2.08 (1)	Fe(2)–C(23)	1.76 (1)
W–S	2.429 (2)	Fe(2)–C(21)	1.79 (1)
W–Fe(2)	2.852 (1)	Fe(2)–C(22)	1.82 (1)
W–Fe(1)	2.854 (1)	Fe(2)–S	2.179 (2)
Fe(1)–C(13)	1.76 (1)	O–C(av)	1.13 (1)

Table IV. Intramolecular Bond Angles (deg) for $Fe_2W(CO)_{11}(\mu_3\text{-}S)$ (**2**)

C(42)–W–S	110.1 (2)	C(12)–Fe(1)–W	109.8 (3)
C(42)–W–Fe(2)	62.7 (2)	S–Fe(1)–Fe(2)	53.87 (6)
C(42)–W–Fe(1)	98.8 (2)	S–Fe(1)–W	55.77 (6)
C(45)–W–S	160.6 (3)	Fe(2)–Fe(1)–W	63.20 (4)
C(45)–W–Fe(2)	146.8 (2)	C(23)–Fe(2)–S	94.5 (4)
C(45)–W–Fe(1)	145.0 (3)	C(23)–Fe(2)–Fe(1)	97.0 (3)
C(44)–W–S	109.1 (2)	C(23)–Fe(2)–W	150.0 (3)
C(44)–W–Fe(2)	100.4 (2)	C(21)–Fe(2)–S	108.1 (3)
C(44)–W–Fe(1)	62.2 (2)	C(21)–Fe(2)–Fe(1)	160.5 (3)
C(41)–W–S	80.8 (3)	C(21)–Fe(2)–W	101.3 (3)
C(41)–W–Fe(2)	128.0 (3)	C(22)–Fe(2)–S	148.9 (3)
C(41)–W–Fe(1)	88.6 (2)	C(22)–Fe(2)–Fe(1)	95.4 (3)
C(43)–W–S	84.5 (2)	C(22)–Fe(2)–W	109.4 (3)
C(43)–W–Fe(2)	89.6 (2)	S–Fe(2)–Fe(1)	53.91 (6)
C(43)–W–Fe(1)	131.4 (2)	S–Fe(2)–W	55.81 (6)
S–W–Fe(2)	47.91 (5)	Fe(1)–Fe(2)–W	63.28 (4)
S–W–Fe(1)	47.91 (5)	Fe(2)–S–Fe(1)	72.22 (8)
Fe(2)–W–Fe(1)	53.51 (3)	Fe(2)–S–W	76.28 (7)
C(13)–Fe(1)–S	95.2 (3)	Fe(1)–S–W	76.32 (7)
C(13)–Fe(1)–Fe(2)	95.1 (3)	O–C–Fe(av)	178 (1)
C(13)–Fe(1)–W	150.1 (3)	O(42)–C(42)–W	167.4 (7)
C(11)–Fe(1)–S	105.5 (3)	O(44)–C(44)–W	167.3 (8)
C(11)–Fe(1)–Fe(2)	158.5 (3)	O(41)–C(41)–W	175.8 (8)
C(11)–Fe(1)–W	101.6 (3)	O(43)–C(43)–W	177.6 (8)
C(12)–Fe(1)–S	151.4 (3)	O(45)–C(45)–W	179 (1)
C(12)–Fe(1)–Fe(2)	98.1 (3)		

groupings. For the compounds **2**, **2a–c**, we believe that a more localized scheme consisting of a series of donor–acceptor bonds, as indicated by the arrows in structure A, has considerable merit.

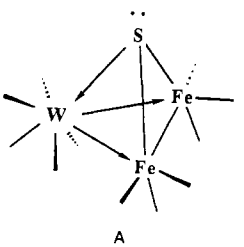

A

In this model, a lone pair of electrons on the sulfido ligand is donated to an empty octahedral-like d^2sp^3 hybrid orbital on the tungsten atom. The tungsten–iron bonds can be viewed as donor–acceptor bonds from the tungsten atom to the iron atoms with the electron pairs originating in the filled unhybridized d orbitals on the $W(CO)_4L$ group. Cotton has shown that the formation of semibridging carbonyl ligands often occurs in the presence of donor–acceptor metal–metal bonds.[28] The development of semibridging character in two of the carbonyl ligands on the $W(CO)_4L$ group is consistent with this bonding model. When one of the CO ligands on tungsten is replaced by a less effective π-back-bonding ligand such as PMe_2Ph, the electrons on the unhybridized d orbitals should become more available for use in bonding to the iron atoms. The shorter length of the tungsten–iron bonds in **2a** is consistent with this interpretation.

An ORTEP drawing of the molecular structure of **3c** is shown in Figure 3. Pertinent intramolecular bond distances and angles are listed in Tables VII and VIII. The cluster consists of a

Table V. Intramolecular Distances (Å) for $Fe_2W(CO)_{10}(PMe_2Ph)(\mu_3\text{-}S)$ (**2a**)

W–C(42)	1.992 (7)	Fe(1)–S	2.196 (2)
W–C(44)	2.026 (7)	Fe(1)–Fe(2)	2.572 (1)
W–C(43)	2.050 (7)	Fe(2)–C(23)	1.767 (7)
W–C(41)	2.059 (7)	Fe(2)–C(21)	1.787 (8)
W–S	2.406 (2)	Fe(2)–C(22)	1.793 (7)
W–P	2.522 (2)	Fe(2)–S	2.178 (2)
W–Fe(1)	2.812 (1)	P–C(38)	1.791 (7)
W–Fe(2)	2.818 (1)	P–C(37)	1.811 (6)
Fe(1)–C(11)	1.764 (8)	P–C(31)	1.812 (6)
Fe(1)–C(13)	1.776 (7)	C–O(av)	1.136 (9)
Fe(1)–C(12)	1.800 (9)	C–C(av)	1.37 (1)

Table VI. Intramolecular Bond Angles (deg) for $Fe_2W(CO)_{10}(PMe_2Ph)(\mu_3\text{-}S)$ (**2a**)

C(42)–W–Fe(1)	62.1 (2)	Fe(2)–Fe(1)–W	62.92 (3)
C(42)–W–Fe(2)	100.3 (2)	C(23)–Fe(2)–Fe(1)	97.6 (2)
C(44)–W–Fe(1)	98.2 (2)	C(23)–Fe(2)–W	149.8 (2)
C(44)–W–Fe(2)	62.5 (2)	C(21)–Fe(2)–Fe(1)	161.1 (2)
C(43)–W–Fe(1)	90.2 (2)	C(21)–Fe(2)–W	100.6 (2)
C(43)–W–Fe(2)	129.0 (2)	C(22)–Fe(2)–Fe(1)	93.1 (2)
C(41)–W–Fe(1)	133.9 (2)	C(22)–Fe(2)–W	108.6 (2)
C(41)–W–Fe(2)	90.0 (2)	S–Fe(2)–Fe(1)	54.31 (6)
S–W–P	160.78 (6)	S–Fe(2)–W	55.81 (5)
S–W–Fe(1)	49.02 (5)	Fe(1)–Fe(2)–W	62.71 (3)
S–W–Fe(2)	48.50 (4)	Fe(2)–S–Fe(1)	72.04 (6)
P–W–Fe(1)	141.66 (4)	Fe(2)–S–W	75.69 (6)
P–W–Fe(2)	147.83 (5)	Fe(1)–S–W	75.19 (6)
Fe(1)–W–Fe(2)	54.37 (3)	O(11)–C(11)–Fe(1)	177.8 (9)
C(11)–Fe(1)–Fe(2)	159.1 (3)	O(12)–C(12)–Fe(1)	177.2 (8)
C(11)–Fe(1)–W	99.9 (2)	O(13)–C(13)–Fe(1)	178.8 (7)
C(13)–Fe(1)–Fe(2)	97.3 (2)	O(21)–C(21)–Fe(2)	177.1 (7)
C(13)–Fe(1)–W	150.7 (2)	O(23)–C(23)–Fe(2)	179.0 (7)
C(12)–Fe(1)–S	152.7 (2)	O(41)–C(41)–W	177.1 (6)
C(12)–Fe(1)–Fe(2)	99.7 (2)	O(44)–C(44)–W	168.7 (6)
C(12)–Fe(1)–W	109.7 (2)	O(22)–C(22)–Fe(2)	177.3 (6)
S–Fe(1)–Fe(2)	53.65 (5)	O(42)–C(42)–W	165.5 (5)
S–Fe(1)–W	55.79 (4)	O(43)–C(43)–W	178.8 (6)

(28) Cotton, F. A. *Prog. Inorg. Chem.* **1976**, *21*, 1.

Table VII. Intramolecular Distances (Å) for $Os_3W(CO)_{11}(PMe_2Ph)_2(\mu_3\text{-}S)$ (**3c**)

Os(1)–C(12)	1.88 (2)	Os(3)–C(32)	1.91 (2)
Os(1)–C(11)	1.89 (2)	Os(3)–W	2.8297 (9)
Os(1)–S	2.314 (4)	W–C(41)	1.98 (2)
Os(1)–P(1)	2.347 (4)	W–C(43)	1.99 (2)
Os(1)–Os(3)	2.8041 (8)	W–C(42)	2.00 (2)
Os(1)–Os(2)	2.837 (1)	W–S	2.365 (4)
Os(1)–W	2.954 (1)	W–P(2)	2.564 (4)
Os(2)–C(21)	1.88 (2)	P(1)–C(58)	1.78 (2)
Os(2)–C(22)	1.89 (2)	P(1)–C(57)	1.79 (2)
Os(2)–C(23)	1.91 (2)	P(1)–C(51)	1.82 (2)
Os(2)–S	2.400 (4)	P(2)–C(68)	1.80 (2)
Os(2)–Os(3)	2.873 (1)	P(2)–C(61)	1.82 (2)
Os(2)–W	2.920 (1)	P(2)–C(67)	1.83 (2)
Os(3)–C(31)	1.86 (2)	O–C(av)	1.16 (2)
Os(3)–C(33)	1.88 (2)	C–C(av)	1.35 (3)

Table VIII. Intramolecular Bond Angles (deg) for $Os_3W(CO)_{11}(PMe_2Ph)_2(\mu_3\text{-}S)$ (**3c**)

C(12)–Os(1)–S	108.9 (4)	C(31)–Os(3)–Os(2)	110.8 (5)
C(12)–Os(1)–P(1)	89.2 (5)	C(33)–Os(3)–Os(1)	107.0 (5)
C(12)–Os(1)–Os(3)	109.9 (4)	C(33)–Os(3)–W	146.6 (5)
C(12)–Os(1)–Os(2)	154.5 (5)	C(33)–Os(3)–Os(2)	85.5 (5)
C(12)–Os(1)–W	94.2 (5)	C(32)–Os(3)–Os(1)	96.1 (4)
C(11)–Os(1)–S	156.3 (6)	C(32)–Os(3)–W	117.4 (5)
C(11)–Os(1)–P(1)	90.2 (5)	C(32)–Os(3)–Os(2)	154.6 (5)
C(11)–Os(1)–Os(3)	73.5 (5)	Os(1)–Os(3)–W	63.23 (2)
C(11)–Os(1)–Os(2)	104.4 (5)	Os(1)–Os(3)–Os(2)	59.95 (2)
C(11)–Os(1)–W	131.6 (5)	W–Os(3)–Os(2)	61.59 (3)
S–Os(1)–P(1)	87.2 (1)	C(41)–W–S	125.3 (5)
S–Os(1)–Os(3)	100.4 (1)	C(41)–W–P(2)	143.9 (6)
S–Os(1)–Os(2)	54.4 (1)	C(41)–W–Os(3)	62.9 (5)
S–Os(1)–W	51.6 (1)	C(41)–W–Os(2)	120.6 (5)
P(1)–Os(1)–Os(3)	155.5 (1)	C(41)–W–Os(1)	79.5 (5)
P(1)–Os(1)–Os(2)	107.3 (1)	C(43)–W–S	98.1 (5)
P(1)–Os(1)–W	137.5 (1)	C(43)–W–P(2)	79.3 (4)
Os(3)–Os(1)–Os(2)	61.23 (2)	C(43)–W–Os(3)	136.1 (4)
Os(3)–Os(1)–W	58.81 (2)	C(43)–W–Os(2)	150.8 (4)
Os(2)–Os(1)–W	60.52 (3)	C(43)–W–Os(1)	106.3 (5)
C(21)–Os(2)–S	132.5 (6)	C(42)–W–S	149.8 (5)
C(21)–Os(2)–Os(1)	136.3 (6)	C(42)–W–P(2)	75.3 (4)
C(21)–Os(2)–Os(3)	78.7 (6)	C(42)–W–Os(3)	88.1 (5)
C(21)–Os(2)–W	88.6 (6)	C(42)–W–Os(2)	108.6 (5)
C(22)–Os(2)–S	125.2 (6)	C(42)–W–Os(1)	146.1 (5)
C(22)–Os(2)–Os(1)	89.9 (6)	S–W–P(2)	82.3 (1)
C(22)–Os(2)–Os(3)	91.9 (6)	S–W–Os(3)	98.4 (1)
C(22)–Os(2)–W	146.1 (6)	S–W–Os(2)	52.7 (1)
C(23)–Os(2)–S	87.5 (6)	S–W–Os(1)	50.1 (1)
C(23)–Os(2)–Os(1)	127.5 (6)	P(2)–W–Os(3)	143.2 (1)
C(23)–Os(2)–Os(3)	173.4 (7)	P(2)–W–Os(2)	94.2 (1)
C(23)–Os(2)–W	121.2 (7)	P(2)–W–Os(1)	132.3 (1)
S–Os(2)–Os(1)	51.63 (9)	Os(3)–W–Os(2)	59.94 (2)
S–Os(2)–Os(3)	96.4 (1)	Os(3)–W–Os(1)	57.96 (2)
S–Os(2)–W	51.7 (1)	Os(2)–W–Os(1)	57.77 (3)
Os(1)–Os(2)–Os(3)	58.82 (2)	Os(1)–S–W	78.3 (1)
Os(1)–Os(2)–W	61.72 (3)	Os(1)–S–Os(2)	74.0 (1)
Os(3)–Os(2)–W	58.48 (3)	W–S–Os(2)	75.6 (1)
C(31)–Os(3)–Os(1)	159.1 (5)	O(41)–C(41)–W	163 (1)
C(31)–Os(3)–W	95.9 (5)	O–C(av)–M	176 (2)

tetrahedrally arranged group of three osmium atoms and one tungsten atom with a triply bridging sulfido ligand on one of the Os_2W triangular faces. The Os–Os bonds are similar to those observed in **4**, which has a similar but much more symmetrical structure. The sulfur-bridged W–Os bonds, W–Os(1) = 2.954 (1) and W–Os(2) = 2.920 (1) Å, are significantly longer than the unbridged bond W–Os(3) = 2.8297 (9) Å. A similar effect was observed for the Os–Os distances in **4**.[29] However, the Os–Os distances in **3c** show considerable scatter. The longest Os–Os bond, Os(2)–Os(3) = 2.873 (1) Å is one of the unbridged bonds. Compound **3c** contains two phosphine ligands. The one coordinated to the tungsten atom was presumably brought into the complex during the addition of the tungsten atom. The second phosphine ligand is coordinated to one of the sulfur-bridged osmium atoms. This ligand was, presumably, derived from $W(CO)_5(PMe_2Ph)$ during the irradiation. Compound **3c** contains 11 carbonyl ligands distributed as shown in Figure 3. All of the carbonyl ligands are of a linear terminal type except for C(41)–O(41), which is a semibridge between W and Os(3), W–C(41)–O(41) = 163 (1)°.

(29) Adams, R. D.; Foust, D. F.; Mathur, P. *Organometallics* **1983**, *2*, 990.

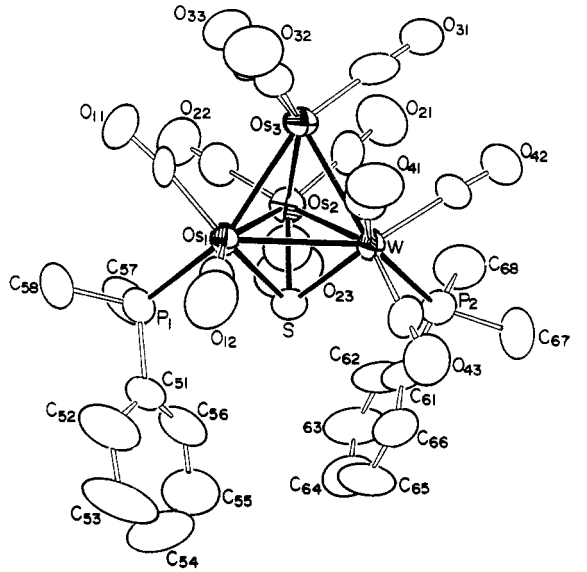

Figure 3. ORTEP drawing of $Os_3W(CO)_{11}(PMe_2Ph)_2(\mu_3\text{-}S)$ (**3c**).

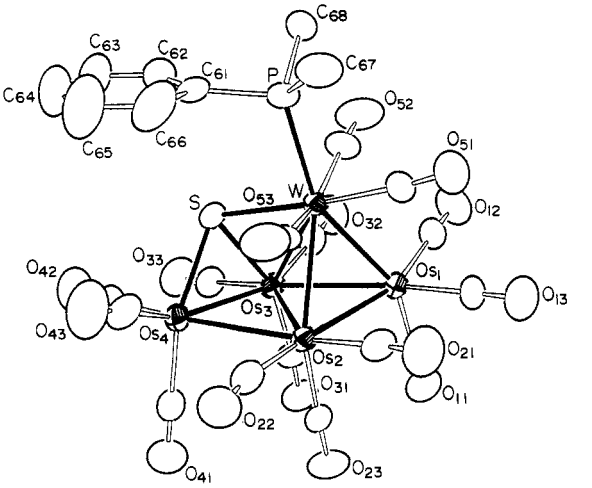

Figure 4. ORTEP drawing of $Os_4W(CO)_{15}(PMe_2Ph)(\mu_3\text{-}S)$ (**5**).

Table IX. Intramolecular Distances (Å) for $Os_4W(CO)_{15}(PMe_2Ph)(\mu_3\text{-}S)$ (**5**)

Os(1)–C(13)	1.86 (1)	Os(3)–Os(4)	2.8053 (7)
Os(1)–C(11)	1.91 (1)	Os(3)–W	2.9455 (8)
Os(1)–C(12)	1.91 (1)	Os(4)–C(42)	1.87 (2)
Os(1)–W	2.7828 (8)	Os(4)–C(43)	1.87 (2)
Os(1)–Os(2)	2.7987 (7)	Os(4)–C(41)	1.90 (1)
Os(1)–Os(3)	2.9515 (8)	Os(4)–S	2.391 (3)
Os(2)–C(23)	1.89 (1)	W–C(51)	1.97 (1)
Os(2)–C(21)	1.90 (1)	W–C(53)	2.02 (1)
Os(2)–C(22)	1.92 (1)	W–C(52)	2.02 (1)
Os(2)–Os(3)	2.8271 (8)	W–S	2.413 (3)
Os(2)–Os(4)	2.8388 (8)	W–P	2.513 (3)
Os(2)–W	2.8870 (8)	P–C(68)	1.79 (1)
Os(3)–C(31)	1.90 (1)	P–C(67)	1.81 (2)
Os(3)–C(33)	1.91 (1)	P–C(61)	1.83 (1)
Os(3)–C(32)	1.92 (1)	C–O(av)	1.14 (1)
Os(3)–S	2.417 (3)		

An ORTEP drawing of the molecular structure of **5** is shown in Figure 4. Intramolecular bond distances and angles are listed in Tables IX and X. The cluster of metal atoms consists of a group of three osmium and one tungsten atom arranged in the form of a tetrahedron with an $Os(CO)_3$ group bridging one of the

Table X. Intramolecular Bond Angles (deg) for $Os_4W(CO)_{15}(PMe_2Ph)(\mu_3\text{-}S)$ (**5**)

C(13)–Os(1)–W	110.8 (4)	S–Os(3)–Os(1)	108.59 (7)
C(13)–Os(1)–Os(2)	106.3 (4)	Os(4)–Os(3)–Os(2)	60.53 (2)
C(13)–Os(1)–Os(3)	164.9 (4)	Os(4)–Os(3)–W	84.34 (2)
C(11)–Os(1)–W	154.3 (4)	Os(4)–Os(3)–Os(1)	117.39 (2)
C(11)–Os(1)–Os(2)	100.7 (4)	Os(2)–Os(3)–W	59.98 (2)
C(11)–Os(1)–Os(3)	93.3 (4)	Os(2)–Os(3)–Os(1)	57.89 (2)
C(12)–Os(1)–W	100.7 (4)	W–Os(3)–Os(1)	56.32 (2)
C(12)–Os(1)–Os(2)	160.6 (4)	C(42)–Os(4)–S	89.2 (4)
C(12)–Os(1)–Os(3)	105.9 (4)	C(42)–Os(4)–Os(3)	103.7 (5)
W–Os(1)–Os(2)	62.30 (2)	C(42)–Os(4)–Os(2)	163.4 (5)
W–Os(1)–Os(3)	61.73 (2)	C(43)–Os(4)–S	103.5 (4)
Os(2)–Os(1)–Os(3)	58.83 (2)	C(43)–Os(4)–Os(3)	153.1 (4)
C(23)–Os(2)–Os(1)	92.5 (4)	C(43)–Os(4)–Os(2)	106.1 (4)
C(23)–Os(2)–Os(3)	94.6 (4)	C(41)–Os(4)–S	159.0 (4)
C(23)–Os(2)–Os(4)	102.2 (3)	C(41)–Os(4)–Os(3)	104.5 (4)
C(23)–Os(2)–W	148.2 (4)	C(41)–Os(4)–Os(2)	87.0 (4)
C(21)–Os(2)–Os(1)	76.7 (4)	S–Os(4)–Os(3)	54.74 (7)
C(21)–Os(2)–Os(3)	139.3 (4)	S–Os(4)–Os(2)	84.10 (7)
C(21)–Os(2)–Os(4)	154.7 (4)	Os(3)–Os(4)–Os(2)	60.11 (2)
C(21)–Os(2)–W	92.0 (4)	C(51)–W–S	172.0 (4)
C(22)–Os(2)–Os(1)	165.9 (4)	C(51)–W–Os(1)	73.1 (4)
C(22)–Os(2)–Os(3)	129.5 (4)	C(51)–W–Os(2)	99.7 (4)
C(22)–Os(2)–Os(4)	70.2 (4)	C(51)–W–Os(3)	135.1 (4)
C(22)–Os(2)–W	118.9 (4)	C(53)–W–S	87.8 (4)
Os(1)–Os(2)–Os(3)	63.28 (2)	C(53)–W–Os(1)	109.5 (3)
Os(1)–Os(2)–Os(4)	121.53 (2)	C(53)–W–Os(2)	59.1 (3)
Os(1)–Os(2)–W	58.58 (2)	C(53)–W–Os(3)	107.4 (3)
Os(3)–Os(2)–Os(4)	59.36 (2)	C(52)–W–S	97.5 (4)
Os(3)–Os(2)–W	62.05 (2)	C(52)–W–Os(1)	86.7 (4)
Os(4)–Os(2)–W	84.83 (2)	C(52)–W–Os(2)	141.4 (4)
C(31)–Os(3)–S	156.3 (4)	C(52)–W–Os(3)	91.5 (4)
C(31)–Os(3)–Os(4)	102.8 (4)	S–W–P	88.8 (1)
C(31)–Os(3)–Os(2)	87.5 (4)	S–W–Os(1)	114.33 (7)
C(31)–Os(3)–W	138.2 (4)	S–W–Os(2)	82.66 (8)
C(31)–Os(3)–Os(1)	85.0 (4)	S–W–Os(3)	52.48 (7)
C(33)–Os(3)–C(32)	89.0 (6)	P–W–Os(1)	154.65 (8)
C(33)–Os(3)–S	83.0 (4)	P–W–Os(2)	138.68 (8)
C(33)–Os(3)–Os(4)	79.9 (4)	P–W–Os(3)	139.07 (8)
C(33)–Os(3)–Os(2)	138.2 (4)	Os(1)–W–Os(2)	59.12 (2)
C(33)–Os(3)–W	132.7 (4)	Os(1)–W–Os(3)	61.95 (2)
C(33)–Os(3)–Os(1)	162.6 (4)	Os(2)–W–Os(3)	57.98 (2)
C(32)–Os(3)–S	105.4 (4)	Os(4)–S–W	107.0 (1)
C(32)–Os(3)–Os(4)	157.2 (4)	Os(4)–S–Os(3)	71.40 (8)
C(32)–Os(3)–Os(2)	132.7 (4)	W–S–Os(3)	75.16 (8)
C(32)–Os(3)–W	88.9 (4)	O(21)–C(21)–Os(2)	173 (1)
C(32)–Os(3)–Os(1)	75.5 (4)	O(22)–C(22)–Os(2)	169 (1)
S–Os(3)–Os(4)	53.87 (8)	O(51)–C(51)–W	173 (1)
S–Os(3)–Os(2)	83.88 (8)	O(53)–C(53)–W	163 (1)
S–Os(3)–W	52.36 (7)	O–C–M(av)	177 (1)

Os–Os edges. A triply bridging sulfido ligand bridges one W–Os edge of the tetrahedral group and one of the Os–Os bonds to the bridging $Os(CO)_3$ group. The tungsten–osmium bond distances span a considerable range: W–Os(1) = 2.7828 (9), W–Os(2) = 2.8870 (8), W–Os(3) = 2.9455 (8) Å. We can offer no rational explanation for this, but the distances are not vastly different from those observed in **3c**. Similarly, the osmium–osmium distances span a wide range, 2.7987 (8)–2.9515 (8) Å, with the greatest differences between the two bonds to Os(1); however, these distances are not unusually long or short. The metal–sulfur bond distances are not unusual and are similar to those in **3c** and other sulfido–tungsten–osmium carbonyl cluster complexes.[30] Four of the carbonyl ligands, C(21)–O(21), C(22)–O(22), C(51)–O(51), and C(53)–O(53), show a semibridging character. The strongest of these is C(53)–O(53) on the tungsten atom; W–C(53)–O(53) = 163 (1)° is associated with the Os(2)–W bond. Although there is reason to formulate the existence of some donor–acceptor bonds in the cluster, vide infra, simple electron counting would not suggest the presence of such a bond to W or Os(2).

Compound **5** contains a total of 74 cluster valence electrons. With this number, each metal atom can achieve an 18-electron configuration. However, with this bonding picture, the Os(4)–S bond would be regarded as a donor–acceptor bond from S to Os(4) and the Os(1)–Os(3) bond would be regarded as a donor–acceptor bond from Os(3) to Os(1). A second structure that is frequently observed for 74-electron cluster complexes containing five metal atoms is the square pyramid, and the related complexes $Os_5(CO)_{15}(\mu_4\text{-}S)$[31] and $Os_4Pt(CO)_{13}(PPh_3)(\mu_4\text{-}S)$[8] both possess the square-pyramidal structure. The reason why **5** does not adopt the square-pyramidal structure also is not clear, but steric crowding of the ligands could be an important factor. For example, the structure of $Os_5(CO)_{15}(\mu_4\text{-}S)$ showed the presence of significant ligand crowding. The addition of another ligand (**5** contains 16) could destabilize the square-pyramidal structure sufficiently to force the metal atoms to adopt an alternative arrangement. The importance of ligand–ligand contacts on cluster geometry has been discussed by Johnson et al.[32]

Conclusions. The bonding of the $W(CO)_4L$ fragments to the clusters **2** and **2a** can be viewed as a combination of electron pair donation from the sulfido ligand to an empty octahedral-like d^2sp^3 orbital on the tungsten atom and a back-donation of electron pairs from two of the unhybridized d orbitals on the tungsten atom to each of the iron atoms to form the tungsten–iron bonds.

Comparison of the structures of **2** and **2a** suggests that stronger metal–metal bonds are formed when a CO ligand is replaced by the poorer π-acceptor and better σ-donor ligand PMe_2Ph. This is consistent with notion of an increased availability of electron density on the tungsten atom for donation in bond formation to the iron atoms. It may also help to explain the fact that we were unable to obtain the ruthenium and osmium homologues of **2**.

The isolation of **3c** from the reaction that yielded **2c** suggests that the formation of **2c** may have proceeded through a higher nuclearity intermediate similar to **3c**. The existence of tungsten–sulfur bonding in **3c** suggests that the tungsten–sulfur interactions were important in its formation. Similar conclusions can be drawn from the results of the reaction of **4** with $W(CO)_5(PMe_2Ph)$ from which the only mixed-metal product was the higher nuclearity compound **5**.

Acknowledgment. These studies were supported by the National Science Foundation under Grant CHE-8612862. NMR measurements were made on a Bruker AM-300 spectrometer purchased with funds from the National Science Foundation under Grant No. CHE-8411172.

Registry No. **1a**, 74520-99-3; **1b**, 105121-22-0; **1c**, 88746-45-6; **2**, 119454-91-0; **2a**, 119454-92-1; **2b**, 119454-93-2; **2c**, 119454-94-3; **3c**, 119454-95-4; **4**, 82080-90-8; **5**, 119480-06-7; **6**, 119454-96-5; $W(CO)_6$, 14040-11-0; $W(CO)_5(PMe_2Ph)$, 42565-94-6; $Fe_3(CO)_{12}$, 17685-52-8; $(CH_2)_2S$, 420-12-2; $Os_3(CO)_{10}(NCMe)_2$, 61817-93-4; Fe, 7439-89-6; Ru, 7440-18-8; Os, 7440-04-2; W, 7440-33-7.

Supplementary Material Available: Tables of crystallographic data, positional parameters, and anisotropic thermal parameters for **2**, **2a**, **3c**, and **5** (19 pages); tables of observed and calculated structure factor amplitudes for all four structural analyses (89 pages). Ordering information is given on any current masthead page.

(30) (a) Adams, R. D.; Horváth, I. T.; Mathur, P. *J. Am. Chem. Soc.* **1984**, *106*, 6292. (b) Süss-Fink, G.; Thewalt, U.; Heinz-Peter, K. *J. Organomet. Chem.* **1984**, *262*, 315.

(31) Adams, R. D.; Horváth, I. T.; Segmuller, B. E.; Yang, L. W. *Organometallics* **1983**, *2*, 1301.

(32) Johnson, B. E.; Benfield, R. E. *Top. Stereochem.* **1981**, *12*, 253.